# Study of deposit associated with discharge in micro-pixel gas chamber

Homma, Yasuhiro ; Ochi, Atsuhiko ; Moriya, Kenji ; Matsuda, Shinji ; Yoshida, Keiichi ; Kobayashi, Seiji

# Study of deposit associated with discharge in Micro Pixel Gas Chamber

Y. Homma [a,*], A. Ochi [b], K. Moriya [c], S. Matsuda [a], K. Yoshida [c] and M. Kobayashi [b]

[a] *The Graduate School of Technology, Kobe University, Kobe 657-8501, Japan*

[b] *The Graduate School of Science, Kobe University, Kobe 657-8501, Japan*

[c] *The Graduate School of Science and Technology, Kobe University, Kobe 657-8501, Japan*

**Abstract**

During the R&D stage of "Micro Pixel Gas Chambers"($\mu$-PIC) operating in $Ar/C_2H_6$ 90/10, we found some deposits associated with discharge on its dielectric substrate (polyimide). The deposits are thought to be a kind of conductive material from the secondary electron images (SEI) from a scanning electron microscope (SEM). Auger electron spectroscopy clearly shows that the main component of the deposits is carbon (98%). To clear the origin of deposits, intentional spark tests are done, in which a single pixel is sparked with a specified number of times. The SEI-images clearly show that discharges occur in narrow gaps between the electrodes. During a test in $Ar/C_2H_6$ 50/50 gas mixture, the amount of carbon deposits depended on the number of spark. Also, a decrease in the applicable voltage after the test was also found to be dependent on the number of spark monotonously. However, in the test in pure $N_2$ gas, no clear deposit was found. These observations suggest that carbon deposits come from ethane dissociated by avalanche UV photons. Even from the spark test in pure $N_2$ gas, a decrease in applicable voltage after the test was observed. This could be attributed to a sort of carbonization of the polyimide surface. Although the SEM-images alone could not show clear proof of this so far, this carbonization seems to contribute much less than $C_2H_6$ dissociation by UV photons.

*Key words:* $\mu$-PIC, MSGC, surface streamer, SEM, radiation damage

*PACS:* 29.40.Cs; 29.40.Gx; 51.50.+v; 52.80.Tn

## 1 Introduction

Recently, gaseous radiation detectors have changed from wire to micro-patterned type, mainly because of the requirement for operation in intense beam conditions. The pioneering work of A. Oed [1] opened a new generation of micro-patterned gas-multiplication radiation detectors. In which some kind of dielectric material is an important component to support the electrode structure. In future high luminosity accelerator experiments, radiation detectors could be exposed to hard radiation background including neutrons or heavily ionized particles. These experiments could cause chamber deterioration. Even wire chambers in present accelerators, commonly deteriorate after long term operation. Gain reduction in wire chambers has been attributed to certain impurities in chamber gasses [2,3] deposited on anode wires. With micro-patterned detectors, there could be new chance that abrupt discharges stimulated by radiation background damage the substrate materials resulting in serious damage to the detectors. Therefore, damage of substrates from radiation is one of the most serious issues that should be investigated in detail. The work of H. S. Cho *et. Al.* [4] shows that electrodes were damaged from sparks intentionally driven in their "Micro Gap Chamber" using a scanning electron microscope (SEM). This was a challenging study to solve the discharge problem the material aspect, although they concentrated on inspection of the anode electrodes. A detailed study by V. Pescov *et. Al.* [5,6] suggests that gain reduction is inevitable in microstrip gas chamber (MSGC)-type structures by a surface streamer [7] generated on the surfaces of dielectric materials. They suggest, mainly from calculation, that the surface streamer originated from an enhanced electric field by a triple dielectric material boundary. Therefore, it is necessary to prove this finding experimentally. However, little investigation about the damages done to materials on a micrometer scale has been done. We used "Micro Pixel Chamber" ($\mu$-PIC), one of MSGC type detectors, for the purpose of this investigation. The $\mu$-PIC[8] has been developed as a versatile radiation detector, and it has already shown its unique functionality in various radiation measurement application[9,10,11]. The most desirable feature of a $\mu$-PIC is its feasibility in commercial production processes. The main structure is produced with print circuit board technology. However, when more sophisticated operations are demanded in some applications that require high gas-gain of over $10^4$, such as the detection of minimum ionization particles or long term stable operations like x-ray detection in space, more knowledge

* Corresponding author. Tel.: +81 78 803 6080; fax: +81 78 803 6080
*Email address:* homma@kobe-u.ac.jp (Y. Homma).

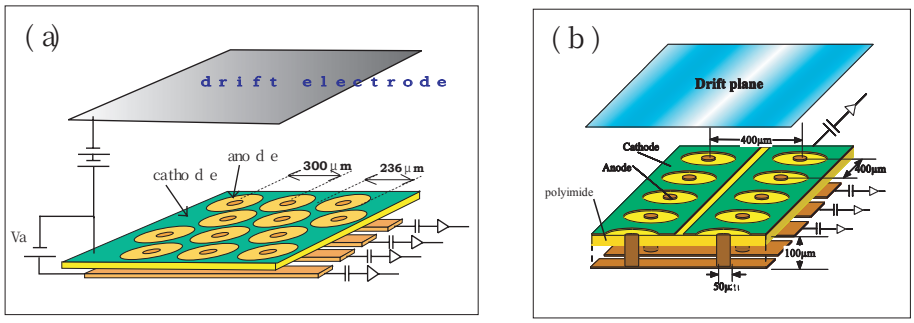


Fig. 1. Schematic drawing of $\mu$-PIC; (a) with hexagonal pixel configuration (H-type) and (b) with matrix pixel configuration (S-type). This type is used for spark test because only a single pixel can be sparked properly.

about a material's discharge property is needed, because a single electric breakdown stimulated by accidental large charge deposits could cause an increase in the dead space region on detectors. In this study, damaged pixels of $\mu$-PIC were studied on a micrometer scale by observing with a SEM, and residuals of pixel damage were investigated systematically using an intentional spark test.

## 2 $\mu$-PIC

We used two types of $\mu$-PICs. The main difference between them was the pixel configuration. The one used for the source test had a hexagonal configuration (Figure 1(a); abbreviated as H-type), anode pitch of 300 $\mu$m, anode diameter of 74 $\mu$m, and a cathode hole diameter of 236 $\mu$m.

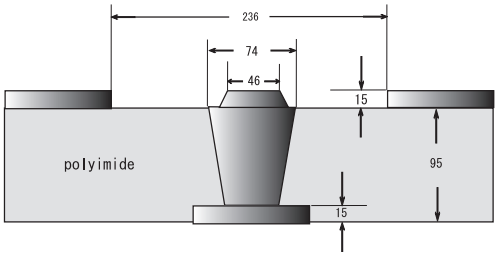


Fig. 2. Dimensions of $\mu$-PIC with hexagonal pixel configuration (H-type). S-type one for spark test was similar. Scale in $\mu$m.

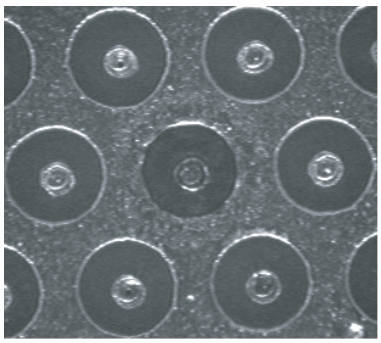

Fig. 3. A microscope image of a damaged pixel. Some hazy material covering the pixel with a little larger circle than that of the pixel (diameter 236$\mu$m) can be observed.

The thickness of the electrode (nickel plated on copper) was 15 $\mu$m (detailed scale is shown in Figure 2) . The other one used for the spark test had a square matrix configuration (abbreviated as S-type). It was possible to spark only a single pixel with an appropriately applied voltage (Figure 1(b)). More detail

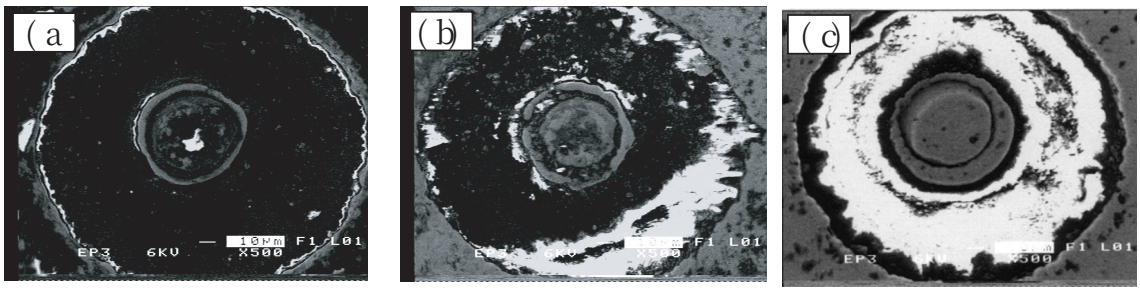


Fig. 4. A microscope image of a damaged pixel. Some hazy material covering the pixel with a little larger circle than that of the pixel (diameter 236$\mu$m) can be observed.

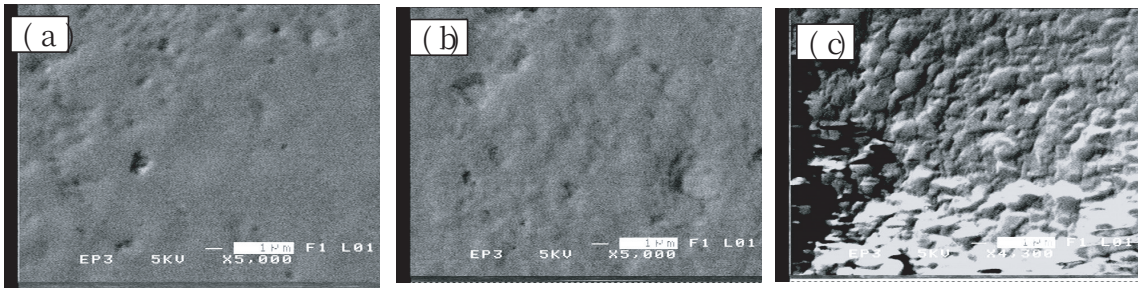


Fig. 5. TOPO-images (magnification $\times$ 5000) of damaged area (a) (b) undamaged area (c). All images are in the same order as the corresponding SEI-images.

is seen in Ref. [8]. Both types of $\mu$-PICs were fabricated using a commercial print circuit board with a polyimide base and with both copper faces covered with an anti-oxidation layer of nickel plating.

## 3 Deposits on damaged pixels

For some tests, $\mu$-PICs , irradiated with an $^{55}$Fe RI source(Mn-K$_\alpha$), with an anode voltage of 500$\sim$550 V, stimulated continuing current flow. Figure 3 shows a typical microscope picture of a damaged pixel. In the center of the image we can see the damaged pixel covered with a hazy material, which forms a little larger circle than the pixel circle. There could be various degrees of damages for each pixel. Figure 4 shows SEI-images for one undamaged pixel (c) and two damaged pixels (a) (b). There are several methods of observing with a SEM. The SEI method is sensitive to insulating surfaces because of electron trapping on the surface of non-conductive specimens (charge up). When a surface has a high resistivity, electrons emitted from the SEM electron gun attach to the surface and then the secondary electron emission from the surface effectively increases. This results in brightening the SEM image in that region with high resistivity. This method is called charge contrast imaging (CCI). For an undamaged pixel, almost the entire surface of the dielectric material (polyimide) is brightened by the charge up (Fig. 4(c)). However, in

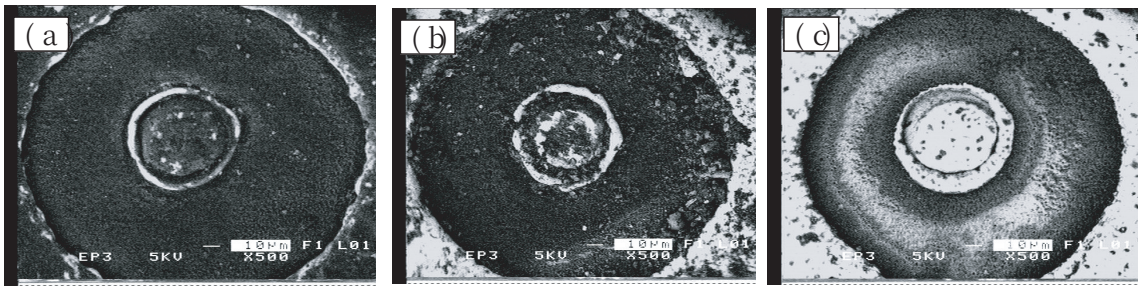


Fig. 6. COMPO-images of damaged (a) (b) and undamaged areas near the damaged pixel (c). Bright area shows metallic composition (Ni plated on Cu). For the damaged pixels, both anodes and cathodes are also covered with light elements. All images are in the same order as the corresponding SEI-images.

Fig. 4(a)(b), most regions are black indicating no electron charge up. For the image of the damaged pixel shown in (b), some areas (lower right) are bright. This shows the tendency of discharge to take place between the narrow electrode gaps (upper left) because of the poor technique in pattern alignment (displacement 12 $\mu$m in average) in the early R&D stages of $\mu$-PIC production. These SEI-images clearly show that certain kinds of conductive materials are deposited on the surface in the case of damaged pixels. We also investigated these deposits using the TOPO-mode of the SEM, which enhances an object's topological variation by scattering electrons with higher energy (more than 50 eV). In Fig. 5 (magnification $\times$ 5000), all the images are aligned in the same order as the corresponding SEI-images. From these images, it is clear that the surfaces of the damaged pixels ( (a), (b) ) are smoothed by grains much smaller than the roughness scale of the polyimide surface of the undamaged pixel (Fig. 5(c)).

## 4 Elements of deposits

We used another mode of the SEM called the COMPO-mode and obtained information about the atomic elements of the deposits. This mode is used to construct an image from scattered electrons with higher energy also. The higher the atomic number, the higher is the reflecting effect of primary high-energy electrons. Figure 6(c) shows the COMPO-image of the undamaged pixel near the damaged pixel. Both the cathode and anode surface are bright suggesting metallic surface. However, in the COMPO-image of the damaged pixel in Fig. 6(a), almost the entire pixel surface, even the cathode and anode surface, are black. For the damaged pixel in Fig. 6(b), not all its cathode surface is bright suggesting few deposits of light atomic elements. Moreover, to identify the atomic composition of the deposits, the sample labelled (a) (in Figs. 4$\sim$6) was subjected to Auger electron spectroscopy (AES). The two 100 $\mu$m$^2$ regions (boxes shown in Fig. 7(a) SEM view) are the inspected points. In Fig. 7(b), the Auger electron spectrum is shown. The upper right point

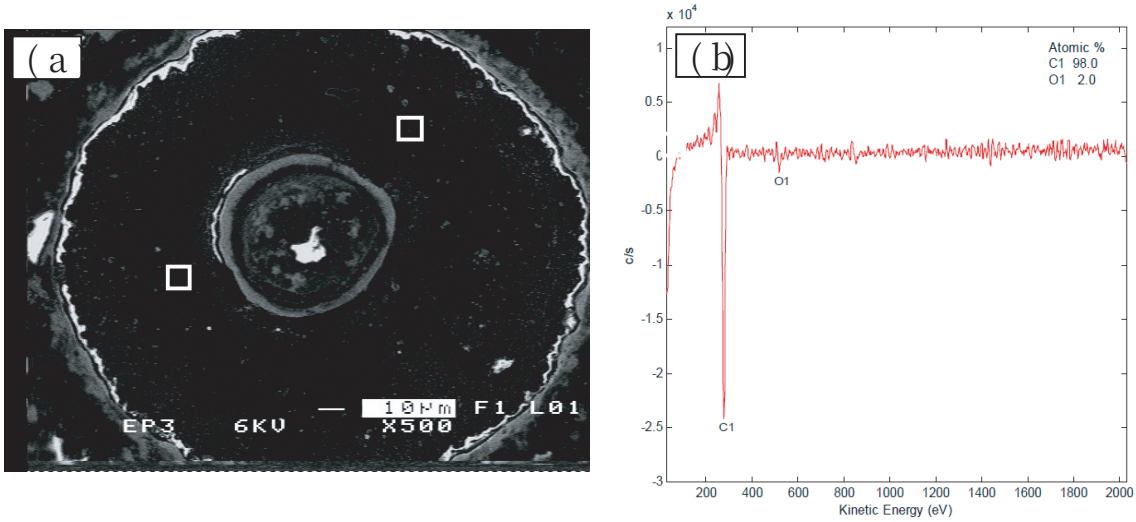


Fig. 7. Auger electron spectroscopy; (a) two 100 $\mu$m$^2$ regions are the inspected points, (b) Auger electron spectrum for the upper right point ( spectrum obtained for the lower left point is almost the same).

(Almost the same spectrum was obtained in lower left point. ) shows 98% carbon atoms and 2% oxygen atoms. It should be noted that no nitrogen, which exists in polyimide, was identified in these spectra.

## 5 Spark test

A spark test was done to investigate the mechanism of carbon deposition on a polyimide surface. The idea is that the amount of deposits will depend on the number of discharges (discharges). Therefore it is essential to stimulate a spark on a single definite pixel. For this purpose a $\mu$-PIC with a square matrix pixel configuration (S-type) was used. Only a pixel with the properly applied voltage to its anode and cathode stimulated a spark. We identified each spark by a flash of light observed through microscope. Each trip of a high voltage power supply, set at a 1 mA current limit, corresponded to each spark. Recovery of high voltage power supply from the trip state was done automatically except in the case of five sparks, where the trip was recovered manually. The energy of each spark was fed through a capacitor with 2000 pF.

Table 1 summarizes the test. The test was conducted in a $Ar/C_2H_6$ 50/50 gas packed plastic container for five pixels (labelled C1∼C5) with different numbers of discharges. The oxygen content was maintained under 0.12% during the entire experiment. After accomplished definite number of discharges, all samples were subjected to an SEM observation. The SEM images of the five pixels with different numbers of discharges in a $Ar/C_2H_6$ 50/50 mixture are

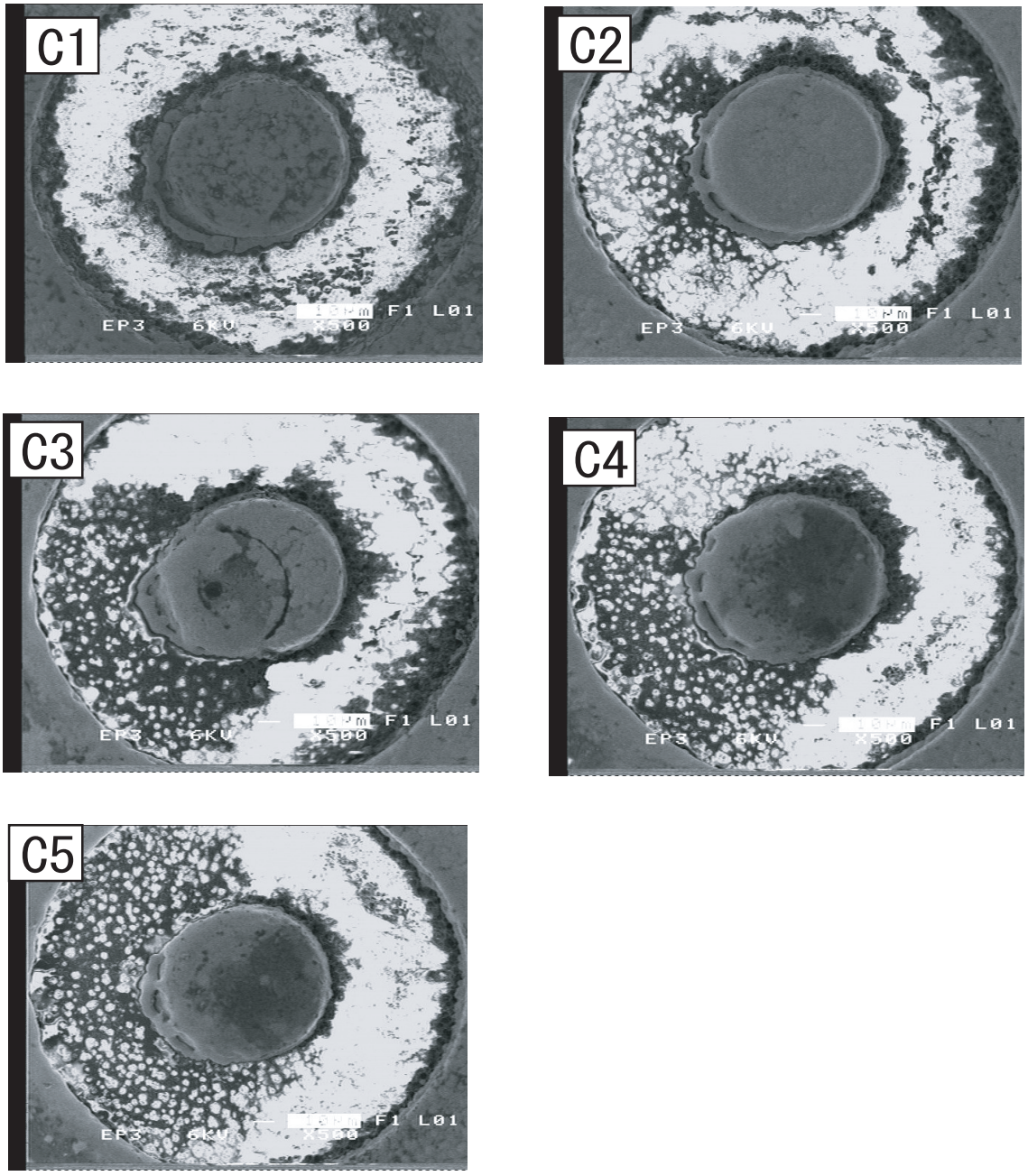


Fig. 8. SEI-images after discharging a definite number of times (5 for C1; 50 for C2; 150 for C3; 250 for C4 and 300 for C5) in $Ar/C_2H_6$ 50/50. Black area tends to increase with number of discharges. Spark gaps were mostly in the lower left electrode gap in the test. It should be noted that each pixel shown is a different one.

Table 1
Summary of spark test. Pixels labelled C1∼C5 tested in $Ar/C_2H_6$ 50/50. "Start voltage" is the anode voltage when the test started and "end voltage" is the anode voltage after the test finished.

| Pixel label | Number of discharges | Start voltage(V) | End voltage(V) |
|---|---|---|---|
| C1 | 5 | 780 | 720 |
| C2 | 50 | 790 | 680 |
| C3 | 150 | 770 | 480 |
| C4 | 200 | 740 | 430 |
| C5 | 300 | 770 | 340 |

shown in Fig. 8. Some deformation in the anode shapes in these images has no relation with the sparks; just a poor production process.

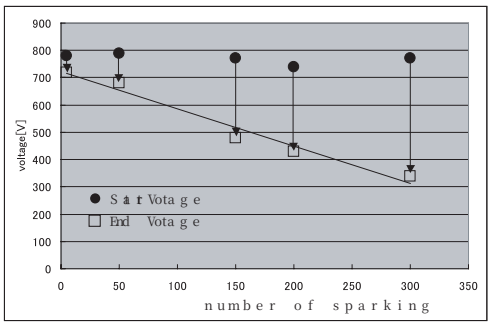


Fig. 9. Applicable voltage drop caused by spark test. Black circles show "start voltage". Squares show "end voltage". The dependency of decreasing in the applicable voltage on number of discharge is clear.

A gradual increase in the black area on the polyimide surface are shown. Fig. 9 shows the dependency of the applicable high voltage after the spark test. The dependency of the decrease in the applicable voltage on the number of discharges was observed.

## 6 Discussions

We discuss the damages of the $\mu$-PIC pixels, which are believed to be inevitable in MSGC type detectors because of surface streamer [7]. To separate the original deposits from $Ar/C_2H_6$ ,/a spark test in pure $N_2$ gas was conducted for three pixels. The summary is shown in Table. 2. At first, the COMPO-images (Fig. 10) show no metallic components, such as Ni or Cu, on the surface. Therefore, no melting or evaporation of metal from $\mu$-PIC electrode occurred. In Fig. 11, the SEM-images of 200 sparks in $Ar/C_2H_6$ 50/50 (a) and those of $N_2$ (b) (c) (d) are shown . Sparks constantly occurred between the narrow anode-cathode gaps; lower left for N6, upper left for N7,

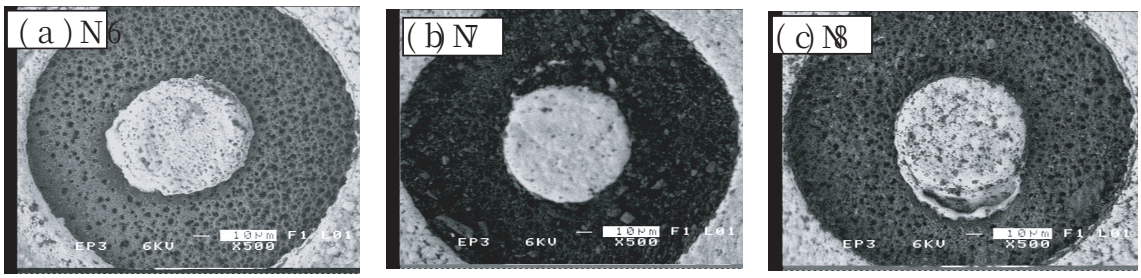


Fig. 10. COMPO-images of pixels after spark test in $N_2$ gas. No metallic component (such as Ni or Cu) on the surface was observed.

lower right for N8 [1] . No apparent and stable black areas was observed in $N_2$ compared with those in $Ar/C_2H_6$ 50/50 though some black or gray areas were observed because of the unstable nature of the charge up. However voltage drops were observed in all three pixels tested in $N_2$ (Table. 2); pixel N6 50% drop, pixel N7 7% drop, and pixel N8 10% drop. The drop in pixel N6 is comparable to or more than that in $Ar/C_2H_6$ 50/50. In Fig. 12, the TOPO-images of pixel N6 are shown; (a) magnification ($\times$ 500), (b) damaged area by higher magnification ($\times$ 5000), (c) undamaged area in the same pixel by higher magnification ($\times$ 5000). Some smoothing in the damaged area (lower left) was observed compared to that in the undamaged area in the same pixel. This could be due to carbon deposits. As carbon could not have come from the gas, this voltage drop in $N_2$ could be an inherent character of the $\mu$-PIC pixels against sparks. Therefore, the cause of some of the degradation in the applicable anode voltage after the test might be a kind of carbonization of the polyimide surface. Why did we not observe any apparent black areas in the SEI-images in the case of $N_2$ compared with the one in $Ar/C_2H_6$ 50/50 although the voltage drop in $N_2$ was greater than that in $Ar/C_2H_6$ 50/50? To explore this observation, two more pixels (N7 and N8) were subjected to the same spark test. But no clear deposits were observed from the SEM-images. However a few percentages in drop off were observed (Tab. 2). It seems to be that N6 was an extreme case. This might be attributed to the localization of the deposits in case of $N_2$ comparing in case of $Ar/C_2H_6$ 50/50. To be clear about this hypothesis, it will be useful to measure local surface conductivity using AFM probing. Here we should note the difference between the source and spark tests on the degree of discharges. In the case of damages in source test, the TOPO-images showed deposits of small grains on the polyimide surface as discussed in the previous section (Fig. 5). And electron avalanche region is expected to be more extended to the drift plane region (Fig. 1) than the region stimulated by the spark test.

We could say that the total amount of deposits in the source test was much larger than that in that in the spark test. These are seen on anode tops in the

[1] The positions of these spark gaps did not have any special meaning. It was for convenient the SEM observation.

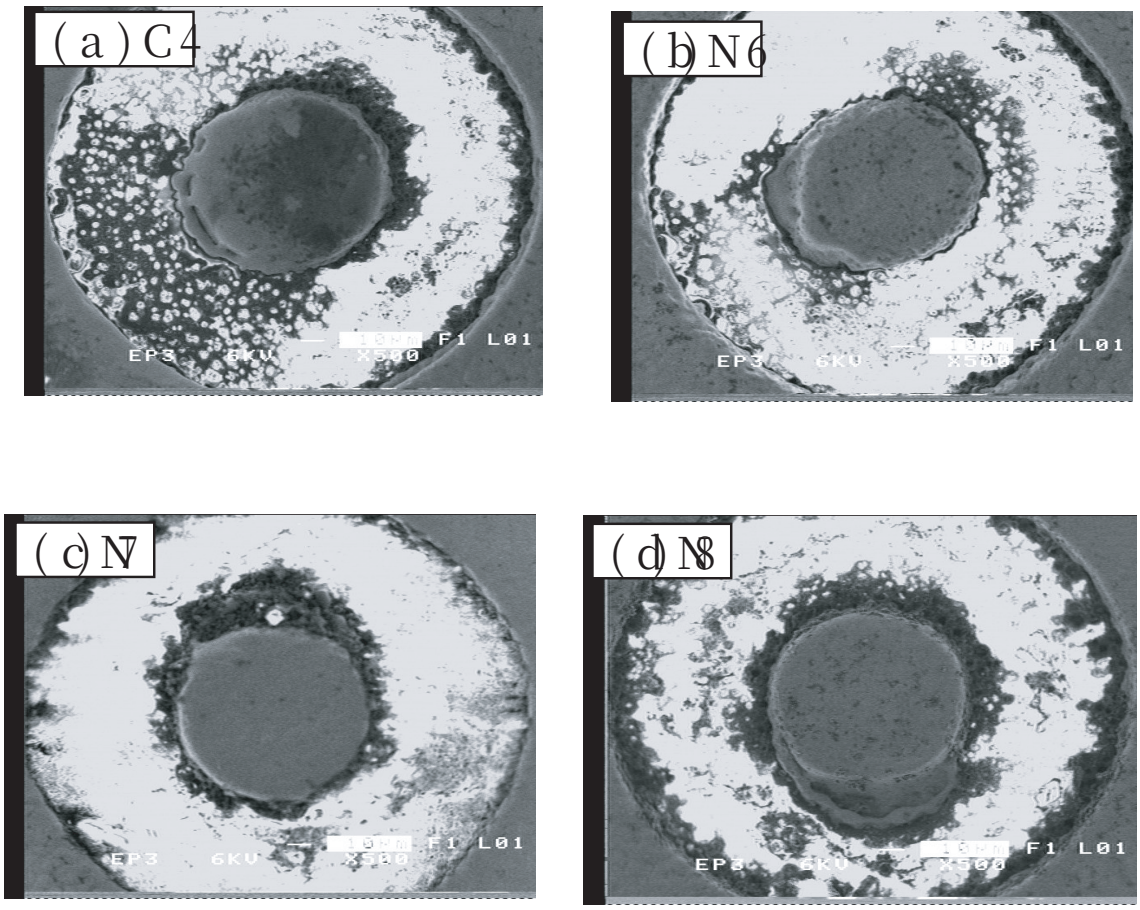


Fig. 11. SEI-images of pixels after the 200 discharges in $Ar/C_2H_6$ 50/50 (a) and in $N_2$ gas (b)∼(d).

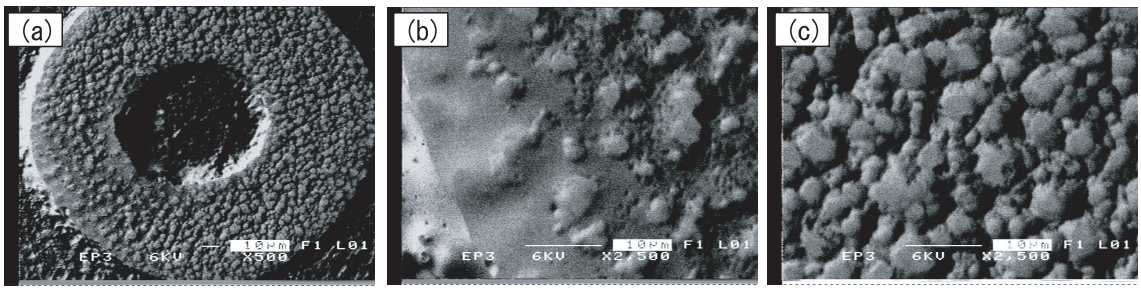


Fig. 12. TOPO-images of pixel N6 after 200 discharges in $N_2$ gas; (a) magnification ($\times$ 500), (b) higher magnification ($\times$ 5000), (c) the undamaged area on the same pixel.

Table 2
Summary of spark test in $N_2$. "Start voltage" is the anode voltage when the test started, and "end voltage" is the anode voltage after the test finished. The number of discharges was fixed at 200 for comparison with the test in $Ar/C_2H_6$ 50/50.

| Pixel label | Number of discharges | Start voltage(V) | End voltage(V) |
|---|---|---|---|
| N6 | 200 | 760 | 380 |
| N7 | 200 | 820 | 760 |
| N8 | 200 | 620 | 560 |

spark test with pixels C3∼C5. This also shows that the majority of deposits observed in Fig. 5(a), covering the entire pixel region including the anode top, is from dissolved $C_2H_6$. From the viewpoint of material science, this process reminds us of the plasma-process in atmospheric pressure, which extends its applicable field for large-scale thin film production [13]. There are various types of carbon deposits, from amorphous to diamond like carbon (DLC). The best experimental method to survey this is Raman spectroscopy. But because of the strong luminescence from the substrate (polyimide) itself, the Raman peak could not be identified in our experiment so far.

## 7 Summary

Using the secondary electron imaging (SEI) method of SEM, we observed conductive deposits on the dielectric material (polyimide) surface of damaged $\mu$-PIC pixels which discharged in the operation tests in $Ar/C_2H_6$ 90/10. The main component of the deposits is thought to be carbon judging from the SEM-images (SEI,TOPO and COMPO modes). The Auger electron spectrum clearly verifies this observation (98% carbon). About 2% of the oxygen in the deposits is thought to come from water in atmosphere during storage. Therefore, the deposits on the damaged pixels are composed purely of carbon. We conclude they come from hydrocarbons ($C_2H_6$), which are dissolved by UV photons. The spark test in $Ar/C_2H_6$ 50/50 clearly shows the dependence of deposits on the number of discharges. A similar test done in pure $N_2$ gas shows some decrease in the applicable anode voltage after the spark test. This might be the inherent character of the $\mu$-PIC pixel structure to discharge and might show some carbonization of the polyimide surface. No melting or evaporation of metal from the $\mu$-PIC electrode was observed in the damaged pixels in both the source and spark tests using the composition imaging method in SEM. This research shows the first direct observation of damage features in MSGC-type radiation detectors.

## Acknowledgements

We would like to show our great appreciation to Prof. Tanimori and the members of the Cosmic Ray Laboratory at Kyoto University. We would also like to express our gratitude to the staff and students in the Particle Physics Laboratory at Kobe University.

## References

[1] A.OED, Nucl. Instr. Meth. A 263 (1988) 351.

[2] R. Openshaw, R. S. Henderson, W. Frazer and M. Salomon, Nucl. Instr. Meth. A 307 (1991) 298.

[3] K.Abe et al., IEEE Trans. on Nucl. Scin. 45(3) (1998) 648.

[4] H. S. Cho, N. Palaio, W. S. Hong, J. Kadyk, V. Perez-Mendez and J. Vujic, IEEE Trans. on Nucl. Scin. 45(3) (1998) 280.

[5] V. Peskov, B. D. Ramsey, P. Fonte, IEEE Trans. Nucl. Scin. 45(3) (1998) 244.

[6] V.Peskov, B. D. Ramsey, J. J. Kolodziejczak, P. Fonte, Nucl. Instr. Meth. A 397 (1997) 243.

[7] V. Peskov, B. D. Ramsey, P. Fonte, Nucl. Instr. Meth. A 392 (1997) 89.

[8] A. Ochi, T. Nagayoshi, S. Koishi, T. Tanimori, T. Nagae and M. Nakamura, Nucl. Instr. Meth. A 471 (2001) 264.

[9] H. Kubo, K. Miuchi, T. Nagayoshi, A. Ochi, R. Orito, A. Takada, T. Tanimori and M. Ueno, Nucl. Instr. Meth. A 513 (2003) 94.

[10] T. Nagayoshi, S. Koishi, H. Kubo, K. Miuchi, R. Orito, A. Takada, A. Takeda, T. Tanimori, M. Miura, O. Bouianov and M. Bouianov, Nucl. Instr. Meth. A 525 (2004) 20.

[11] S. Kabuki et al., Nucl. Instr. Meth. A 580 (2007) 1031.

[12] P. Fonte, V. Peskov, B. D. Ramsey, Nucl. Instr. Meth. A 416 (1998) 23.

[13] Japanese patent No. 2005-298286.